

SCIENTIFIC REPORTS

OPEN

Low-energy band structure and even-odd layer number effect in AB-stacked multilayer graphene

Ryuta Yagi¹, Taiki Hirahara¹, Ryoya Ebisuoka¹, Tomoaki Nakasuga¹, Shingo Tajima¹, Kenji Watanabe^{1,2} & Takashi Taniguchi²

How atoms acquire three-dimensional bulk character is one of the fundamental questions in materials science. Before addressing this question, how atomic layers become a bulk crystal might give a hint to the answer. While atomically thin films have been studied in a limited range of materials, a recent discovery showing how to mechanically exfoliate bulk crystals has opened up the field to study the atomic layers of various materials. Here, we show systematic variation in the band structure of high mobility graphene with one to seven layers by measuring the quantum oscillation of magnetoresistance. The Landau fan diagram showed distinct structures that reflected differences in the band structure, as if they were finger prints of multilayer graphene. In particular, an even-odd layer number effect was clearly observed, with the number of bands increasing by one for every two layers and a Dirac cone observed only for an odd number of layers. The electronic structure is significantly influenced by the potential energy arising from carrier screening associated with a gate electric field.

Since the discovery of graphene¹, various theoretical and experimental studies have been carried out to elucidate its nature^{2–9}. Moreover development of techniques to produce high-quality graphene^{10–13} with sufficiently long mean free paths has made it possible to study ballistic transport^{14–16} and to modify band structures by using moiré structures created by the slight misalignment of bilayer honeycomb lattices of graphene and *h*-BN¹⁷. Since the beginning of research on graphene, the electronic band structure of this material has been expected to show a particular layer number dependence^{18–24}. Even if we consider only AB-stacking, the band structure should show an even-odd layer number effect^{20–22,24}, as shown in Fig. 1a: the band structures of $2N$ and $2N + 1$ ($N = 1, 2, 3, \dots$) layer graphene show N bilayer-like bands with non-zero band mass, and the $2N + 1$ layer additionally shows a monolayer-like band that is massless with a linear dispersion relation. To date, optical measurements of the band structure have been performed on graphene consisting of several numbers of layers^{25–28}. However, the low-energy band structure, which affects transport properties, has been only studied for samples consisting of a few layers, by measuring the response of the resistance to gate voltage in the absence of a magnetic field^{29–31}, and from quantum oscillation in magnetic fields^{1,32–34}. In this study, we studied the electronic band structure of high-quality samples of graphene consisting of one to seven layers by measuring quantum oscillations and found systematic variations in the band structure.

Results

Sample characterization. Figure 1b and c show the schematic structures of the samples and an optical micrograph of a typical sample. Graphene was formed on a high quality *h*-BN flake^{11,12}, which has an atomically flat surface, or encapsulated with *h*-BN flakes¹³. The number of layers and stacking were determined by examining the G' peak appearing at approximately 2700 cm^{-1} in the Raman spectra³⁵, topography obtained using an atomic force microscope, and color intensity analysis of a digitized optical micrograph (see the Supplementary Information). The Raman G' peak for AB-stacked graphene exhibited a systematic variation with the numbers of layers^{28,35}, as shown in Fig. 1d. We measured the Raman spectra for many graphene flakes. The shapes of the G' peaks were reproducible from sample to sample and consistent with the reports from other groups^{35,36}, except for an offset in the background signal and slight offset in the Raman shift. This enabled us to accurately determine the number of layers and stacking. The carrier density was varied using a back gate built using a conducting Si substrate covered with its oxide¹. Typical electrical mobilities ranged between $30,000$ and $100,000\text{ cm}^2/\text{Vs}$.

¹Graduate School of Advanced Sciences of Matter, Hiroshima University, Kagamiyama Higashihiroshima, Hiroshima, 739-8530, Japan. ²National Institute for Material Science (NIMS), Namiki, Tsukuba, 305-0044, Japan. Correspondence and requests for materials should be addressed to R.Y. (email: yagi@hiroshima-u.ac.jp)

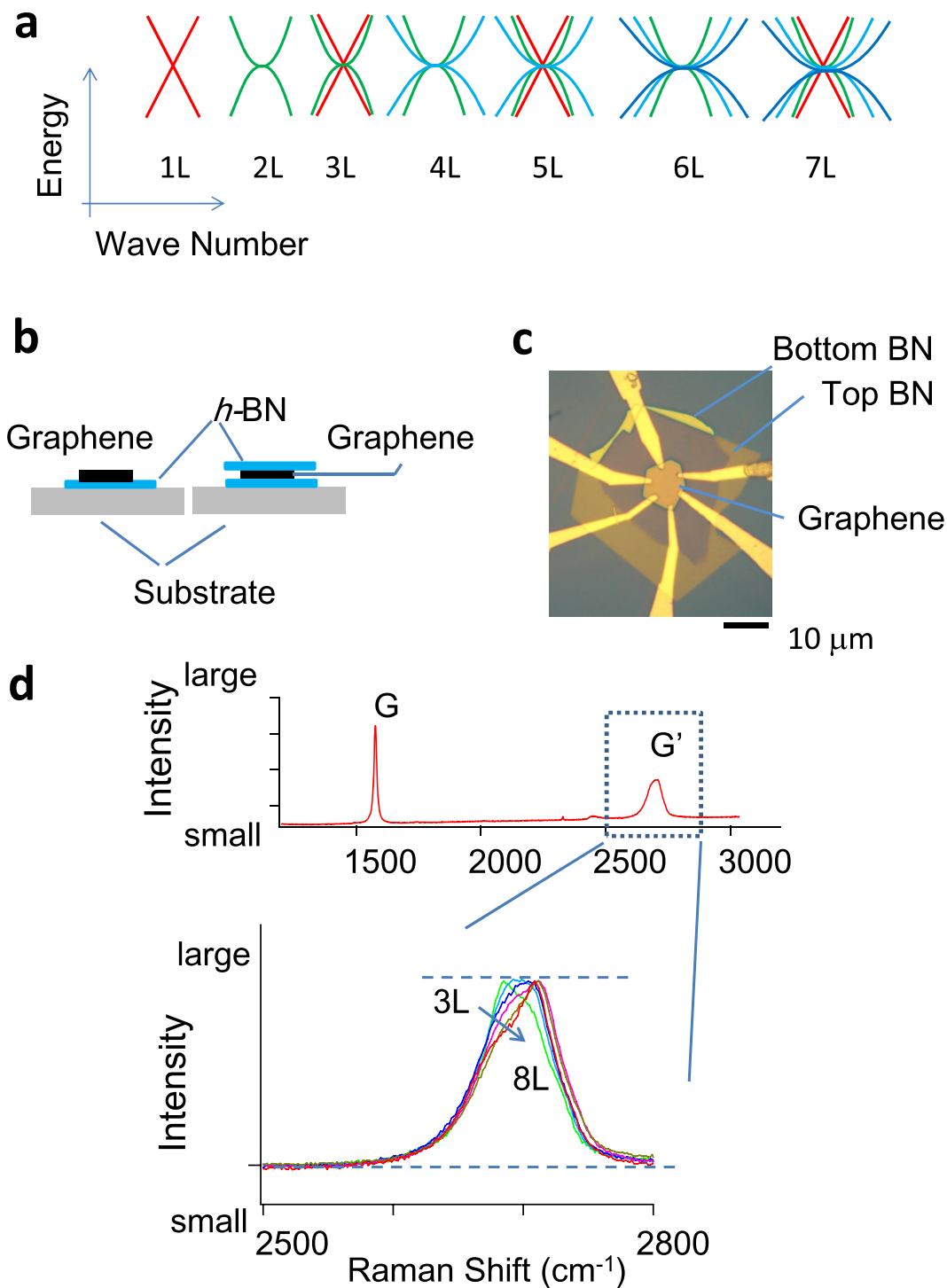


Figure 1. Sample characterization. (a) Schematic diagram of the band structure of AB-stacked graphene. (b) Sample structure. Some graphene samples were encapsulated with *h*-BN flakes. Other samples were not encapsulated but transferred onto the top of a thin *h*-BN flake. (c) Optical micrograph of a typical encapsulated sample. (d) (Top) Example of Raman spectra. (Bottom) Variation in Raman G' band spectra in AB-stacked graphene with increasing layer number from 3 to 8. Data are scaled and offset to better compare the shapes of the peaks.

Landau fan diagram. Low-temperature magnetoresistance measurements showed Shubnikov-de Haas (S-dH) oscillations arising from Landau quantization. Figure 2 shows mappings of the derivative of magnetoresistance (dR_{xx}/dB) for samples with one to seven layers, as a function of gate voltage and magnetic field. These fan diagrams appear to be the finger-prints of graphene as to its specific layer number and stacking because

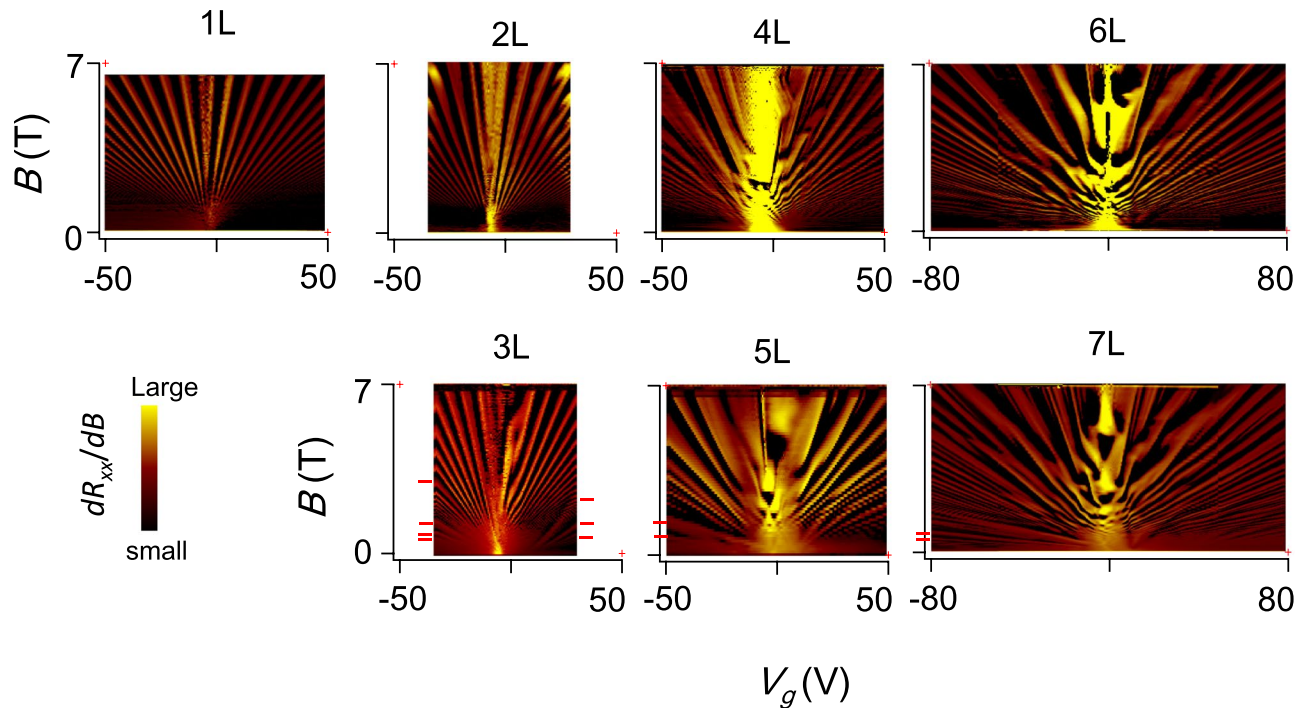


Figure 2. Landau fan diagram. Landau fan diagram for AB-stacked graphene. Measurements were carried out at $T = 4.2$ K. The derivative of the transverse resistivity with respect to the magnetic field is plotted on a color scale as a function of the total carrier density which was tuned by the gate voltage. To improve visibility the cube root of $\frac{dR_{xx}}{dB}$ is plotted. Red marks indicate the positions of the peaks arising from monolayer bands.

they reflect specific band structures. In particular, the streaks and bright spots arise from the Landau levels and their crossings. They vary strikingly with the number of layers and directly reflect different electronic structures. Although the results for samples with one to four layers have been already reported in the literature^{32–34,37,38}, we will briefly review their features here to discuss the systematic variation of the electronic structure in multilayer graphene. As shown in Fig. 2, mono- and bi-layer graphene have simple fan-shaped structures^{1,37,38} because they have a set of Landau levels for an electron band and a hole band. The fan-shaped diagram for the monolayer originates from the fact that each Landau levels has a degeneracy of $4eB/h$. The monolayer and the bilayer are similar to each other but different in terms of the zero-mode Landau levels that appear at the charge neutrality point near $V_g \approx 0$ V: the degeneracy for bilayer graphene is twice that for a monolayer¹, and it manifests itself as a difference in the widths of the zero-mode Landau levels. Trilayer graphene shows one fan-shaped structure arising from bilayer graphene, as well as a monolayer band whose Landau levels can be seen at low magnetic fields³². The Landau levels of the monolayer bands appearing in the fan diagram are quite different from those found in in monolayer graphene. Since monolayer and bilayer bands in trilayer graphene show different dispersion relations, the carrier density in the monolayer band is much less than that in the bilayer bands. Therefore, the Landau levels of the monolayer band reach the quantum limit at much lower magnetic fields compared to the bilayer band. For four or more layers, *i.e.*, $N \geq 4$, Landau fan diagrams become increasingly complicated with increasing number of layers. As can be seen in the figure, bright spots and streaks near the charge neutrality point form complicated patterns, which differ layer to layer. This variation probably originates from the fact that the Landau level structures are different for different layer numbers. Despite their complexity, we could find monolayer bands at odd layer numbers at low magnetic fields, as indicated by red marks in the figure. In the hole regime, (*i.e.*, $n_{osc} < 0$) conspicuous streaks are observed at low magnetic fields. However, in the electron regime, one can discern streaks corresponding to monolayer bands only in trilayer graphene. This electron-hole asymmetry in the band structure arises possibly from the energy offset at the bottoms of the bands. These monolayer bands do not appear for even layers, *i.e.*, two, four and six-layer graphene.

FFT results. The pattern that grows in complexity with increasing layer number in the vicinity of $n_{tot} = 0$ is possibly due to the formation of semi-metallic band structures because the Landau level crossings originate from electron and hole bands that are offset in energy. Here we will not go into the details of these structures, which will be reported elsewhere. Rather, we will discuss the general features of the band structure by taking the Fourier transform of the S-dH oscillation. The Landau level structure away from the charge neutrality point is rather simple, which enables us to obtain physical insights by estimating the number of bands and their dispersions. S-dH oscillations are periodic against the reciprocal of the magnetic fields and their period $\Delta(1/B)$ is relevant to the area A of the energy contour (Fermi surface) of a band, from which the carrier density can be calculated using the formula, $n_{osc} = 4 \times A / (2\pi)^2 = 4(e/h) / \Delta(1/B)$. We employed a fast Fourier transform (FFT) to observe the periodicity. Figure 3 shows the Fourier spectra as a function of the total carrier density n_{tot} induced by the back-gate voltage.

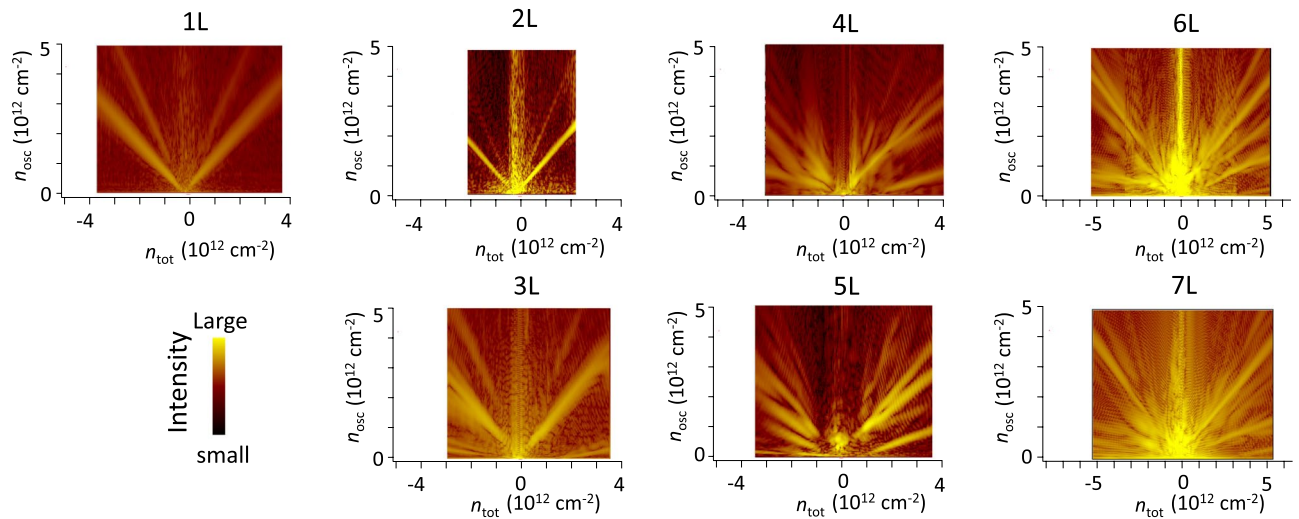


Figure 3. Carrier density of each band. FFT spectra of magnetoresistance plotted against total carrier density n_{tot} . The magnitude of the spectra is plotted with color. The frequency of the FFT (vertical axis) has been converted to have dimensions of carrier density.

Here the total carrier density was calculated using calibrated gate capacitances, and the FFT frequency was scaled by a factor of $4(e/h)$, which directly indicates the carrier density for low energy bands in graphene. In the figure, some noticeable spectra that reflect the carrier density of the Fermi surfaces appear at a given chemical potential tuned by the gate voltage. Other peaks can be assigned to higher-order harmonics whose frequencies can be expressed as multiples of the base frequency or their sums (see the Supplementary Information). These samples show a characteristic layer number dependence. It is clear that FFT spectra for samples with $2N$ and $2N + 1$ ($N = 1, 2, 3$) layers are somewhat similar to each other in terms of the n_{tot} dependence of n_{osc} except for the presence of bands with a small carrier density in odd layers. This should occur because $2N$ and $2N + 1$ layer graphene have N bilayer bands: for example, two and three layer each have one bilayer band, four and five layer graphene each have two bilayer bands, *etc.* Reflecting dispersion relations, the density of states of the monolayer band is much less than that of bilayer bands. The relative intensity of the S-dH oscillation arising from the monolayer band decreased as the layer number increased. This is because the carrier density of the monolayer band is reduced because the number of bilayer bands is increased.

In addition to this even-odd layer number effect relevant to the monolayer band, there are small differences in the n_{osc} of bilayer bands between the samples with $2N$ and $2N + 1$ ($N = 1, 2, 3$) layers. This difference partly stems from the dependence of the band mass on the layer number; although the number of bilayer bands in $2N$ layers equals that of $2N + 1$ layers, values of the mass in those bands are expected to be slightly different²². Moreover the difference can also result from the fact that the energy offset value of each band is somewhat dependent on the layer number²⁰.

Discussion

Theoretical calculation and screening of gate potential. We performed a calculation based on the tight-binding model. A simple calculation of the dispersion relation using all the Slonczewski-Weiss-McClure (SWMcC) parameters of graphite could approximately explain the experimental result obtained for $N < 4$. However for $N \geq 4$, the disagreement became progressively larger as the layer number increased (see the Supplementary Information). Fine tuning of the SWMcC parameters did not significantly change the situation. Much better agreement between experiment and calculation was obtained when the potential due to screening by gate induced carriers was considered. Figure 4 shows the results. In our experiment, the carrier density was tuned by the external gate voltage. This is basically equivalent to the behavior of a capacitor formed by the graphene, insulator (h -BN), and gate electrode. A simple capacitor model tells us that the induced charge is located at the surface of the metals and that there are no electric fields inside the gate electrode. However, in the case of an atomic layer material, one must take screening of the induced charge into account, as was discussed in refs^{27,39–41}. Hence in the calculation, we assumed screening of the form $\propto \exp(-d/\lambda)$ where λ is the screening length and d is distance from the surface. The parameter λ was adjusted so that calculations fit the experiments (see the Supplementary Information). The effect of screening becomes increasingly evident as the layer number increases. The screening lengths are equivalent to approximately one to two layers, which approximately agrees with the theoretically predicted value⁴¹.

Since the beginning of graphene research, there have been investigation into screening of gate induced carriers^{27,40,41}, and the short screening lengths of a few layers have been regarded as having an effect on the electronic property of multilayer graphene⁴². Since the screening length has been expected to be equivalent to approximately a few layers in multilayer graphene, it was assumed that only a few layers could be measured if one used gate electrodes to vary the carrier density of the samples⁴². However, our observations show an even-odd layer number effect and number-of-layers-dependent fan diagrams, which reflects the particular electronic band structures of graphene consisting of four to seven layers. We speculate that these findings indicate that, for at least up to seven

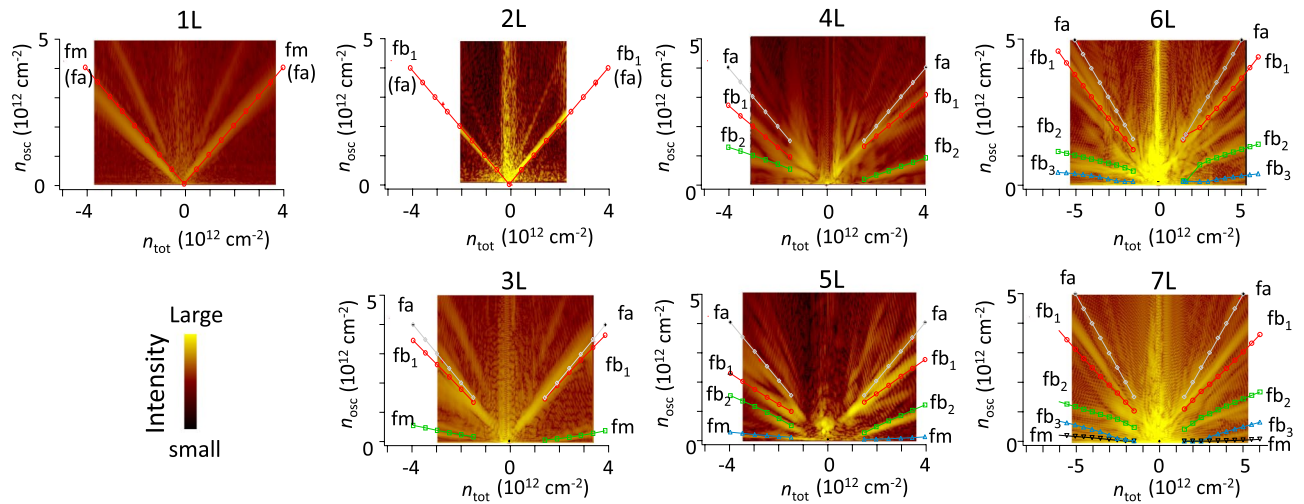


Figure 4. Comparison with band calculation. The dependence of n_{osc} on total carrier density n_{tot} for each band was calculated for graphene with three to seven layers using a Hamiltonian based on the effective mass approximation. The results are displayed as symbols, while the lines are guides for the eye. Carrier density was calculated from the energy contour of the dispersion relation at zero magnetic field. The SWMcC parameters for this calculation were $\gamma_0 = 3$ eV, $\gamma_1 = 0.45$ eV, $\gamma_2 = -0.023$ eV, $\gamma_3 = 0.3$ eV, $\gamma_4 = 0.04$ eV, $\gamma_5 = 0.04$ eV, and $\Delta' = (\Delta - \gamma_2 + \gamma_5) = 0.032$ eV. Screening length λ was 0.33, 0.33, 0.33, 0.43, and 0.35 nm for layers three to seven, respectively. The SWMcC parameters for this calculation better reproduced the experimental results compared to the parameters used for graphite. The peaks for the bilayer are labeled as fb_1 , fb_2 , and fb_3 . The peak of the monolayer band is labeled fm .

layers, coherent quantum states associated with the band structure form along the layer direction, *i.e.*, perpendicular to the sample plane, even in the presence of a gate induced potential variation.

The present results answer the question of how graphene becomes graphite as the layer numbers increases. Generalizing this argument, we can conclude that monolayer bands exist even in graphene with larger numbers of odd layers, and presumably even in graphite as long as AB-stacking is preserved in the entire sample and that the number of layers is odd. However, finding a monolayer band would become increasingly difficult because of the large number of bilayer bands.

On other stackings and other systems. We have limited our concern to band structures in AB-stacked graphene. For a layer number larger than 2, ABC-stacking, which is not equivalent to ABA-stacking, is possible and is expected to show different band structures. The number of possible stacking increases with the number of layers. Each stacking is expected to show different band structures^{24,43}. Some of these band structures with small layer numbers have been identified from optical measurements. However, transport experiments have only been carried out for ABC-stacked trilayer graphene^{31,44}. Further studies of graphene with various layer stackings will contribute to a comprehensive understanding of the transition from atomic layers to the bulk.

A layer number dependence in the electronic band structures was also reported in metal dichalcogenides: the energies of the bottoms of the band were found to vary systematically with the number of layers^{45–47}. Moreover, a similar but different even-even odd layer number effect was recently observed in MoS₂ atomic layer devices⁴⁸; the reported Landau levels showed a valley Zeeman effect in samples with odd layer numbers, and a spin Zeeman effect in samples with even layer numbers. Another example is the topological insulator Bi₂Se₃. Topologically protected surface states, which appear in the bulk, showed mixing as the number of layers decreases⁴⁹. Hence, more interesting phenomena might exist that relate atomic layers and bulk materials.

Summary

Shubnikov-de Haas oscillations in AB-stacked graphene with one to seven layers were reported. Graphene exhibited characteristic Landau level structures in the fan diagram, which reflected the dependence of the electronic states on the number of layers. FFT analysis of the periodicity in the $1/B$ -dependence of the magnetoresistance revealed a systematic change in the band structures; in particular, an even-odd layer number effect relevant to the electronic band structure was observed, where a linear band was observed only in odd-layer graphene. The band structure became more sensitive to the gate electric field as the layer number increased.

Methods

Graphene samples are mechanically exfoliated from Kish graphite. The graphene is then transferred onto a thin *h*-BN flake, which was prepared by mechanically exfoliating a high quality *h*-BN crystal. Some samples are encapsulated with *h*-BN flakes. Graphene samples were patterned by using electron beam lithography. Electric resistance measurements were carried out using a standard lock-in technique. Magnetic fields were applied by using a superconducting solenoid.

References

- Novoselov, K. S. *et al.* Two-dimensional gas of massless Dirac Fermions in graphene. *Nature* **438**, 197–200 (2005).
- Castro Neto, A. H., Guinea, F., Peres, N. M. R., Novoselov, K. S. & Geim, A. K. The electronic properties of graphene. *Rev. Mod. Phys.* **81**, 109–162 (2009).
- Das Sarma, S., Adam, S., Hwang, E. H. & Rossi, E. Electronic transport in two-dimensional graphene. *Rev. Mod. Phys.* **83**, 407–470 (2011).
- Geim, A. K. & Novoselov, K. S. The rise of graphene. *Nature Mat.* **6**, 183–191 (2007).
- Novoselov, K. S. *et al.* Room-temperature quantum Hall effect in graphene. *Science* **315**, 1379–1379 (2007).
- Tikhonenko, F. V., Kozikov, A. A., Savchenko, A. K. & Gorbachev, R. V. Transition between electron localization and antilocalization in graphene. *Phys. Rev. Lett.* **103**, 226801 (2009).
- Gorbachev, R. V. *et al.* Detecting topological currents in graphene superlattices. *Science* **346**, 448–451 (2014).
- Young, A. F. & Kim, P. Quantum interference and Klein tunnelling in graphene heterojunctions. *Nature Phys.* **5**, 222–226 (2009).
- Efetov, D. K. *et al.* Specular interband Andreev reflections at van der Waals interfaces between graphene and NbSe₂. *Nature Phys.* **12**, 328–U162 (2016).
- Crossno, J. *et al.* Observation of the Dirac fluid and the breakdown of the Wiedemann–Franz law in graphene. *Science* **351**, 1058–1061 (2016).
- Zomer, P. J., Dash, S. P., Tombros, N. & van Wees, B. J. A transfer technique for high mobility graphene devices on commercially available hexagonal boron nitride. *Appl. Phys. Lett.* **99**, 232104 (2011).
- Dean, C. R. *et al.* Boron nitride substrates for high-quality graphene electronics. *Nature Nanotechnol.* **5**, 722–726 (2010).
- Wang, L. *et al.* One-dimensional electrical contact to a two-dimensional material. *Science* **342**, 614–617 (2013).
- Taychatanapat, T., Watanabe, K., Taniguchi, T. & Jarillo-Herrero, P. Electrically tunable transverse magnetic focusing in graphene. *Nature Phys.* **9**, 225–229 (2013).
- Chen, S. W. *et al.* Electron optics with p–n junctions in ballistic graphene. *Science* **353**, 1522–1525 (2016).
- Yagi, R. *et al.* Ballistic transport in graphene antidot lattices. *Phys. Rev. B* **92**, 195406 (2015).
- Ponomarenko, L. A. *et al.* Cloning of Dirac Fermions in graphene superlattices. *Nature* **497**, 594–597 (2013).
- Wallace, P. R. The band theory of graphite. *Phys. Rev.* **71**, 622–634 (1947).
- McCann, E., Abergel, D. S. L. & Fal'ko, V. I. Electrons in bilayer graphene. *Solid State Commun.* **143**, 110–115 (2007).
- Partoens, B. & Peeters, F. M. From graphene to graphite. *Phys. Rev. B* **74**, 075404 (2006).
- Latil, S. & Henrard, L. Charge carriers in few-layer graphene films. *Phys. Rev. Lett.* **97**, 036803 (2006).
- Koshino, M. & Ando, T. Orbital Diamagnetism in multilayer graphenes. *Phys. Rev. B* **76**, 085425 (2007).
- Nakamura, M. & Hirasawa, L. Electric transport and magnetic properties in multilayer graphene. *Phys. Rev. B* **77**, 045429 (2008).
- Min, H. K. & MacDonald, A. H. Chiral decomposition in the electronic structure of graphene multilayers. *Phys. Rev. B* **77**, 155416 (2008).
- Sprinkle, M. *et al.* First direct observation of a nearly ideal graphene band structure. *Phys. Rev. Lett.* **103**, 226803 (2009).
- Mak, K. F., Lui, C. H., Shan, J. & Heinz, T. F. Observation of an electric-field-induced band gap in bilayer graphene by infrared spectroscopy. *Phys. Rev. Lett.* **102**, 256405 (2009).
- Ohta, T. *et al.* Interlayer interaction and electronic screening in multilayer graphene investigated with angle-resolved photoemission spectroscopy. *Phys. Rev. Lett.* **98**, 206802 (2007).
- Mak, K. F., Shan, J. & Heinz, T. F. Electronic structure of few-layer graphene. *Phys. Rev. Lett.* **104**, 176404 (2010).
- Craciun, M. F. *et al.* Trilayer graphene is a semimetal with a gate-tunable band overlap. *Nature Nanotechnol.* **4**, 383–388 (2009).
- Zhu, W. J., Perebeinos, V., Freitag, M. & Avouris, P. Carrier scattering, mobilities, and electrostatic potential in monolayer, bilayer, and trilayer graphene. *Phys. Rev. B* **80**, 235402 (2009).
- Jhang, S. H. *et al.* Stacking-order dependent transport properties of trilayer graphene. *Phys. Rev. B* **84**, 161408 (2011).
- Taychatanapat, T., Watanabe, K., Taniguchi, T. & Jarillo-Herrero, P. Quantum Hall effect and Landau-level crossing of Dirac Fermions in trilayer graphene. *Nature Phys.* **7**, 621–625 (2011).
- Grushina, A. L. *et al.* Insulating state in tetralayers reveals an even-odd interaction effect in multilayer graphene. *Nature Commun.* **6**, 6419 (2015).
- Wu, Z. F. *et al.* Detection of interlayer interaction in few-layer graphene. *Phys. Rev. B* **92**, 075408 (2015).
- Ferrari, A. C. *et al.* Raman spectrum of graphene and graphene layers. *Phys. Rev. Lett.* **97**, 187401 (2006).
- Lui, C. H. *et al.* Imaging stacking order in few-layer graphene. *Nano Lett.* **11**, 164–169 (2011).
- Bolotin, K. I., Ghahari, F., Shulman, M. D., Stormer, H. L. & Kim, P. Observation of the fractional quantum Hall effect in graphene. *Nature* **462**, 196–199 (2009).
- Bao, W. Z. *et al.* Magnetoconductance oscillations and evidence for fractional quantum Hall states in suspended bilayer and trilayer graphene. *Phys. Rev. Lett.* **105**, 246601 (2010).
- Visscher, P. B. & Falicov, L. M. Dielectric screening in a layered electron gas. *Phys. Rev. B* **3**, 2541 (1971).
- Guinea, F., Castro Neto, A. H. & Peres, N. M. R. Electronic states and Landau levels in graphene stacks. *Phys. Rev. B* **73**, 245426 (2006).
- Koshino, M. Interlayer screening effect in graphene multilayers with ABA and ABC stacking. *Phys. Rev. B* **81**, 125304 (2010).
- Morozov, S. V. *et al.* Two-dimensional electron and hole gases at the surface of graphite. *Phys. Rev. B* **72**, 201401 (2005).
- Koshino, M. & McCann, E. Multilayer graphenes with mixed stacking structure. *Phys. Rev. B* **87**, 045420 (2013).
- Zou, K., Zhang, F., Capp, C., MacDonald, A. H. & Zhu, J. Transport studies of dual-gated ABC and ABA trilayer graphene. *Nano Lett.* **13**, 369–373 (2013).
- Mak, K. F., Lee, C., Hone, J., Shan, J. & Heinz, T. F. Atomically thin MoS₂. *Phys. Rev. Lett.* **105**, 136805 (2010).
- He, J. G., Hummer, K. & Franchini, C. Stacking effects on the electronic and optical properties of bilayer transition metal dichalcogenides MoS₂, MoSe₂, WS₂, and WSe₂. *Phys. Rev. B* **89**, 075409 (2014).
- Calandra, M., Mazin, I. I. & Mauri, F. Effect of dimensionality on the charge-density wave in few-layer 2H-NbSe₂. *Phys. Rev. B* **80**, 241108 (2009).
- Wu, Z. F. *et al.* Even-odd layer-dependent magnetotransport of high-mobility Q-valley electrons in transition metal disulfides. *Nature Commun.* **7**, 12955 (2016).
- Zhang, Y. *et al.* Crossover of the three-dimensional topological insulator Bi₂Se₃ to the two-dimensional limit. *Nature Phys.* **6**, 584–588 (2010).

Acknowledgements

This work was supported by MEXT KAKENHI Grant Number JP25107003.

Author Contributions

R.Y. conceived the experiments. K.W. and T.T. made the high-quality h-BN crystals. H.T., R.E., T.N. and S.T. made the graphene samples. R.Y., H.T., R.E., T.N. and S.T. carried out low-temperature experiments. R.Y. analyzed the data and calculated the band structure. R.Y. wrote the manuscript.

Additional Information

Supplementary information accompanies this paper at <https://doi.org/10.1038/s41598-018-31291-y>.

Competing Interests: The authors declare no competing interests.

Publisher's note: Springer Nature remains neutral with regard to jurisdictional claims in published maps and institutional affiliations.



Open Access This article is licensed under a Creative Commons Attribution 4.0 International License, which permits use, sharing, adaptation, distribution and reproduction in any medium or format, as long as you give appropriate credit to the original author(s) and the source, provide a link to the Creative Commons license, and indicate if changes were made. The images or other third party material in this article are included in the article's Creative Commons license, unless indicated otherwise in a credit line to the material. If material is not included in the article's Creative Commons license and your intended use is not permitted by statutory regulation or exceeds the permitted use, you will need to obtain permission directly from the copyright holder. To view a copy of this license, visit <http://creativecommons.org/licenses/by/4.0/>.

© The Author(s) 2018